doi: 10.1111/j.1420-9101.2009.01845.x

Allometry and performance: the evolution of skull form and function in felids

G. J. SLATER & B. VAN VALKENBURGH

Department of Ecology and Evolutionary Biology, University of California, Los Angeles, CA, USA

Keywords:

allometry;
bite force;
Felidae;
finite element analysis;
gape;
performance;
predation;
skull strength.

Abstract

Allometric patterns of skull-shape variation can have significant impacts on cranial mechanics and feeding performance, but have received little attention in previous studies. Here, we examine the impacts of allometric skull-shape variation on feeding capabilities in the cat family (Felidae) with linear morphometrics and finite element analysis. Our results reveal that relative bite force diminishes slightly with increasing skull size, and that the skulls of the smallest species undergo the least strain during biting. However, larger felids are able to produce greater gapes for a given angle of jaw opening, and they have overall stronger skulls. The two large felids in this study achieved increased cranial strength by increasing skull bone volume relative to surface area. Allometry of skull geometry in large felids reflects a trade-off between the need to increase gape to access larger prey while maintaining the ability to resist unpredictable loading when taking large, struggling prey.

Introduction

As animals increase in body size, either through ontogeny or phylogeny, they tend to change in shape (Thompson, 1942; Gould, 1966, 1977; Schmidt-Nielsen, 1984; Wayne, 1986). Allometric differences, particularly those among closely related species, often directly relate to performance requirements, defined as the ability of an organism to carry out behaviours or tasks that impact fitness (Arnold, 1983; Wainwright, 1994). For example, a large animal requires proportionately thicker limbs to support its body mass compared to a smaller animal. In this simple case, allometric variation is accounted for by general scaling laws, because limb cross-sectional area, the biomechanically important parameter for limb strength, scales to body mass$^{2/3}$ (Schmidt-Nielsen, 1984). In other cases, it is more difficult to directly relate allometry to organismal performance. This is particularly true for structures, such as the cranium, that have multiple functions. In such cases, the significance of allometry can be investigated by examining how allometric variation impacts variables that may be important for organismal performance, such as those related to feeding and acquiring prey (e.g. Emerson *et al.*, 1994).

In this study, we provide such a test using cranial morphology in the cat family (Felidae). Cranial shape in felids exhibits an allometric pattern of variation, with positive allometry of the facial skeleton, relative to the neurocranium. Larger felids therefore exhibit longer facial skeletons than small felids (Slater & Van Valkenburgh, 2008). Cranial allometry in felids may be related to how they capture and kill prey, as well as differences in prey size. All felids are obligate hypercarnivores, meaning that they consume vertebrate flesh almost exclusively (Van Valkenburgh, 1988). Preferred prey size among felids primarily correlates with the size of the felid itself; large cats take proportionately larger prey than small cats, and prey mass often exceeds predator mass in the largest felids (Radloff & Du Toit, 2004; Hayward & Kerley, 2005; Meachen-Samuels & Van Valkenburgh, 2009). This seems to relate to increased energetic requirements in predators larger than a threshold mass of 21 kg (Carbone *et al.*, 1999). Prey is typically killed using a single bite to the back of the neck or throat (Ewer, 1973; Leyhausen, 1979). Previous authors have

Correspondence: Graham. J. Slater, Department of Ecology and Evolutionary Biology, University of California, Los Angeles, 621 Charles E. Young Drive South, Los Angeles, CA, 90095-1606, USA.
Tel.: (310) 825 4669; fax: (310) 206 0484; e-mail: gslater@ucla.edu

hypothesized that large cats should exhibit wider gapes for killing larger prey (Kiltie, 1984, 1988), increased bite forces for subduing large prey (Christiansen, 2008), and stronger crania to resist greater bite forces and struggling prey (McHenry *et al.*, 2007). Until now, no study has specifically investigated the relationship between allometry of cranial form and these important variables for predatory performance in felids.

We investigated the performance implications of allometric skull-shape variation in felids by using linear morphometrics and finite element analysis (FEA). We tested hypotheses relating to three specific performance criteria that may affect predatory performance in felids: (i) does positive allometry of the facial skeleton allow large felids to open their jaws relatively wider?; (ii) do large felids produce relatively greater bite forces than small felids? and (iii) are the skulls of long-faced large felids stronger than those of short-faced small felids? To answer these questions, we first evaluated scaling of gape distance using linear measurements from museum specimens of 29 felid species. We then constructed FE models for three taxa (African wild cat, *Felis lybica*; clouded leopard, *Neofelis nebulosa*; lion, *Panthera leo*) that span the full range of felid body sizes and skull shapes (Slater & Van Valkenburgh, 2008). Unlike many previous comparative FE studies, models were appropriately scaled prior to analysis using a newly developed method (Dumont *et al.*, 2009) that allows for clearer determination of the relationship between shape and performance.

Methods

Gape

We investigated how gape distance, the distance between the tips of the upper and lower canine teeth when the mouth is open, scales with body size using linear morphometrics. Gape distance has previously been estimated from dry skulls by manually manipulating specimens until disarticulation of the jaw joint occurs (Christiansen & Adolfssen, 2005). Studies of living felids have concluded that most species open their jaws to a gape angle of approximately 65° (Emerson & Radinsky, 1980). We therefore developed a method to estimate total gape distance using arc length theorem that allowed us to calculate gape distance for a specific gape angle across all species. Note that our method does not take into account additional cranial features that can may enhance gape distance or gape angle, such as a depressed glenoid fossa and a dorsally rotated palate, or changes in muscle insertions/pennation or fibre length that affect muscle stretch (Herring, 1975). Based on our previous work (Slater & Van Valkenburgh, 2008), many of these features covary with both snout length and felid body size, suggesting that our method provides a repeatable, conservative minimum estimate of maximum gape distance in large felids.

We calculated gape distance as

$$\text{Gape distance} = \text{gape arc length} - (\text{upper canine length} + \text{lower canine length}),$$

where

$$\text{Gape arc length} = \text{lower jaw length} \times \text{gape angle}$$

Jaw length is the distance from the mandibular condyle to the anterior border of the lower canine, and the 65° gape angle is converted into radians. We subtracted upper and lower canine lengths from gape arc length to generate a total gape distance between the tips of the upper and lower canines, thus accounting for positive allometry in tooth length (Van Valkenburgh & Ruff, 1987; Christiansen & Adolfssen, 2005). Measurements were taken from adult museum specimens of 29 felid species with digital calipers, or from lateral and ventral images of felid crania and mandibles with a scale bar, using ImageJ v.1.37 (Rasband, 2006). All measurements were made to 0.01 mm precision. One to five individuals were used for each species (mean = 4), based on availability (Table 1). Only specimens with complete, unworn upper and lower canines were used.

We evaluated scaling of gape distance by using major axis (MA) regression (Warton *et al.*, 2006). Log_{10}-transformed gape values were regressed on $\log_{10}$-basicranial length. We used basicranial length as a body size proxy to avoid confounding effects of jaw length variation that can arise when total skull length or condylobasal length are used in studies of cranial allometry (Radinsky, 1984). The slope of the MA regression was then evaluated against a null hypothesis of isometry (i.e. a slope of 1) by using a slope test (Warton *et al.*, 2006). To account for statistical nonindependence of species, we computed independent contrasts using the topology of Johnson *et al.* (2005). Branch lengths, measured in millions of years, were taken from Johnson *et al.* (2005) and assigned manually in MESQUITE v. 2.6 (Maddison & Maddison, 2009). Contrasts for $\log_{10}$-gape were regressed on positivized contrasts for $\log_{10}$-basicranial length, and the MA slope of the contrast values calculated through the origin (Garland *et al.*, 1992; Warton *et al.*, 2006). Analyses were conducted using the APE (Paradis *et al.*, 2004) and SMATR (Warton *et al.*, 2006) packages for R (R Development Core Team, 2008).

Finite element analysis of bite force and skull strength

We constructed FE models of three felid skulls based on the methods of Dumont *et al.* (2005) and Grosse *et al.* (2007). Only three skulls were included due to the time consuming nature of FE modelling of biological structures. CT scans were used as the basis for the 3D skull models (Table 2). We applied muscle forces over the origins of the temporalis, masseter and pterygoideus

Table 1 Mean (standard deviations) for measurements used in analysis of gape scaling.

Species (*n*)	Jaw length	Basal length	Upper canine	Lower canine	Gape distance
Acinonyx jubatus (5)	112.94 (7.76)	49.15 (3.96)	18.63 (1.82)	15.70 (1.4)	93.80 (7.62)
Caracal aurata (1)	99.67	45.74	16.05	16.78	80.24
Caracal caracal (5)	83.92 (2.55)	35.74 (3.29)	13.88 (0.88)	12.27 (0.85)	69.05 (2.81)
Caracal serval (5)	73.44 (3.49)	32.28 (1.62)	12.96 (0.59)	11.85 (0.76)	58.51 (3.27)
Catopuma temminkii (2)	84.80 (1.32)	40.92 (1.36)	14.94 (0.84)	13.4 (1.10)	67.86 (1.76)
Felis chaus (5)	64.80 (6.33)	30.08 (3.033)	10.97 (0.39)	10.23 (0.94)	52.32 (6.28)
Felis margarita (1)	54.42	28.19	11.16	9.09	41.49
Felis nigripes (2)	50.91 (2.21)	28.30 (0.93)	9.64 (0.81)	8.64 (1.02)	39.48 (0.68)
Felis silvestris (5)	58.21 (5.91)	28.47 (2.53)	10.73 (1.54)	9.73 (1.45)	45.58 (4.07)
Leopardus colocolo (3)	57.37 (2.17)	30.29 (2.59)	10.33 (1.61)	9.44 (1.16)	45.30 (0.54)
Leopardus geofroyyi (5)	57.59 (4.63)	31.77 (2.72)	11.17 (1.38)	10.42 (1.22)	43.73 (3.38)
Leopardus pardalis (4)	82.14 (3.66)	40.61 (3.25)	16.10 (1.60)	14.20 (0.74)	62.89 (2.39)
Leopardus tigrinus (4)	49.59 (4.47)	27.71 (2.19)	8.54 (1.87)	7.72 (1.14)	40.00 (2.03)
Leopardus wiedii (4)	53.76 (1.83)	28.47 (1.57)	9.05 (0.73)	8.97 (0.45)	42.97 (1.12)
Lynx canadensis (5)	77.84 (3.09)	35.06 (1.86)	16.01 (0.99)	15.48 (1.11)	56.83 (2.49)
Lynx rufus (5)	70.90 (5.25)	33.12 (3.48)	13.15 (2.21)	12.71 (1.60)	54.57 (2.66)
Neofelis nebulosa (5)	105.40 (8.73)	46.11 (4.26)	30.11 (2.86)	23.59 (3.41)	65.88 (4.80)
Panthera leo (5)	207.90 (19.52)	84.47 (4.24)	45.78 (4.97)	36.32 (3.02)	153.76 (15.01)
Panthera onca (4)	157.93 (14.57)	69 (5.68)	36.80 (5.59)	31.74 (3.91)	110.63 (9.08)
Panthera pardus (5)	138.02 (16.51)	60.36 (5.52)	32.05 (5.94)	28.74 (3.96)	95.79 (9.30)
Panthera tigris (5)	211.82 (30.13)	74.46 (5.62)	47.79 (3.91)	44.25 (5.32)	148.27 (26.52)
Panthera unica (3)	116.85 (8.69)	47.12 (3.03)	26.09 (2.41)	25.43 (1.89)	81.05 (7.12)
Pardofelis marmorata (5)	61.71 (6.18)	28.31 (2.50)	12.85 (1.34)	11.87 (1.45)	45.29 (5.33)
Prionailurus bengalensis (1)	58.88	28.96	10.31	10.04	46.45
Prionailurus planiceps (5)	62.24 (1.84)	32.32 (0.69)	12.25 (1.06)	11.66 (0.72)	46.70 (0.79)
Prionailurus rubiginosus (3)	49.13 (3.66)	21.93 (1.66)	8.32 (0.70)	7.88 (0.46)	39.55 (23.20)
Prionailurus viverrinus (4)	85.22 (4.66)	41.99 (3.22)	16.36 (1.37)	16.24 (1.52)	64.07 (4.28)
Puma concolor (5)	123.78 (14.35)	56.4 (5.99)	23.56 (4.46)	21.44 (2.87)	95.43 (9.39)
Puma yaguaouroundi (5)	62.37 (3.87)	35.11 (2.16)	10.06 (0.70)	8.67 (0.56)	52.03 (3.36)

Sample sizes (*n*) for each species are indicated in parentheses.

Table 2 Model information for the three finite element models used in this study.

Taxon	Specimen	Slice thickness (mm)	Model size (tet4)	Volume (mm^3)
Felis lybica	LACM 14480	0.28	811162	80411.8
Neofelis nebulosa	USNM 282124	0.25	1030930	119560.7
Panthera leo	MVZ 117849	1.05	1356850	160104.4

muscles using the tangential-plus-normal traction model in the program BoneLoad (Grosse *et al.*, 2007). This method incorporates the effects of muscle wrapping around curved bone surfaces and eliminates artefacts caused by point loads in areas of muscle insertion. Muscle forces were distributed in each model according to percentage contribution of temporalis (64.1%), masseter (28.3%) and pterygoideus (7.6%) to total jaw muscle mass in the jaguar *Panthera onca* (Davis, 1955). Available evidence suggests that these values are fairly consistent across Carnivora (Davis, 1955; Turnbull, 1970).

We controlled for differences in size among the models using a recently developed method for comparing FE models (Dumont *et al.*, 2009). Models were scaled to common surface area (72 067.26 mm^2) and loaded with the same total muscle force (2682 N). In theory, any pair of values can be used, provided the force to surface area ratio is constant among models. We chose these values in order to make the models comparable with those from a previous study of canid skull performance (Slater *et al.*, 2009). The models were assigned homogeneous material properties based on values for domestic dog cortical bone (E = 13.7 GPA, v = 0.3; Cook *et al.*, 1982; Verrue *et al.*, 2001). Including heterogeneous properties for bone has been shown to affect the results of FEAs of skulls (e.g. Strait *et al.*, 2005; McHenry *et al.*, 2007; Wroe *et al.*, 2007b). In this study, we were interested in the relationship between shape and skull performance, rather than the effects of variation in material properties on performance. By modelling skull properties as homogeneous, we were able to interpret differences in performance exclusively in light of differences in cranial shape.

Felids load their skulls in multiple ways during hunting. Biting on restrained prey results primarily in intrinsic loading, where all forces acting on the cranium (e.g. bite forces, jaw reaction forces) are a result of the action of the felid's own jaw musculature. When attempting to capture

prey, additional skull loading will also occur through extrinsic forces generated by the struggling prey. We therefore loaded models to assess their relative performance under these two distinct sets of loading conditions. First, we simulated two intrinsic, muscle-driven loading conditions: bilateral and unilateral canine biting. An axis of rotation extending between the temporomandibular joints was established by constraining one node in the centre of each glenoid fossa. We then applied constraints at the tip of the left canine tooth for unilateral biting and the tips of both canine teeth for bilateral biting. These analyses simulate the loads incurred by the effects of the jaw adducting musculature pulling the skull down onto the constraints at the jaw joints and teeth. We did not model posterior (carnassial or molar) bites as available evidence suggests that felids rely almost exclusively on canine biting during prey capture and killing (Schaller, 1972; Ewer, 1973; Leyhausen, 1979; Bailey, 1993). We then simulated four extrinsic loading conditions: a 'pull back', a 'lateral shake', bilateral canine loading (bending) and unilateral canine loading (torsion). These loads were based on those from published studies (McHenry *et al.*, 2007; Wroe *et al.*, 2007a; Wroe, 2008), although exact model loading and boundary conditions follow those of Slater *et al.* (2009). For each extrinsic load case, 298 N of total force was applied to the models in addition to 2682 N of muscle force as in Slater *et al.* (2009). This ensured that force to surface area ratios were held constant among models within each set of extrinsic load cases, allowing comparison of relative performance among the three taxa. Linear static FE analyses for intrinsic and extrinsic load cases were completed using Strand7 (Strand7 Pty Ltd, Sydney, Australia).

We evaluated performance of the three felid crania based on three criteria. First, we determined how skull shape affects bite performance by comparing average canine bite forces for a given muscle effort from the intrinsic analyses. Because all models were scaled to a common surface area and used equal muscle forces, our null hypothesis was that bite forces should be identical among the three models. Any differences in bite forces could then be interpreted as the result of differences in skull geometry alone (Dumont *et al.*, 2009; Slater *et al.*, 2009). Second, we assessed strength of the skull models under intrinsic and extrinsic loading conditions by comparing model stress, measured as Von Mises stress (Dumont *et al.*, 2005). Bone is an elastic material and therefore fails under a ductile, rather than brittle model of fracture (Nalla *et al.*, 2003). Von Mises stress is a scalar function of the principle stresses at each element and provides a good predictor of failure due to ductile fracture (Dumont *et al.*, 2005). Lower stress values and more even stress distributions were interpreted as indicating stronger structures for a given loading condition. Finally, we assessed the work efficiency of the skull models by comparing total strain energy values, a measure of energy lost to deformation. In terms of work efficiency, optimal structures are those that maximize stiffness for a given volume of material (Dumont *et al.*, 2009). Lower strain energy values indicate stiffer structures and therefore greater work efficiency. Strain energy values were corrected for differences in volumes of the models using Equation 5 from Dumont *et al.* (2009). Our null hypotheses for all analyses were that stress and strain energy values should be identical among scaled models.

Results

Gape

The MA slope of $\log_{10}$-gape distance on $\log_{10}$-basicranial length was 1.149 (95% CIs: 1.046–1.22) and was significantly > 1 (slope test, $r = 0.506$, $P = 0.005$; Fig. 1a). The MA slope of phylogenetically independent contrasts was 1.139 (95% CIs: 1.002–1.295), also indicating a trend

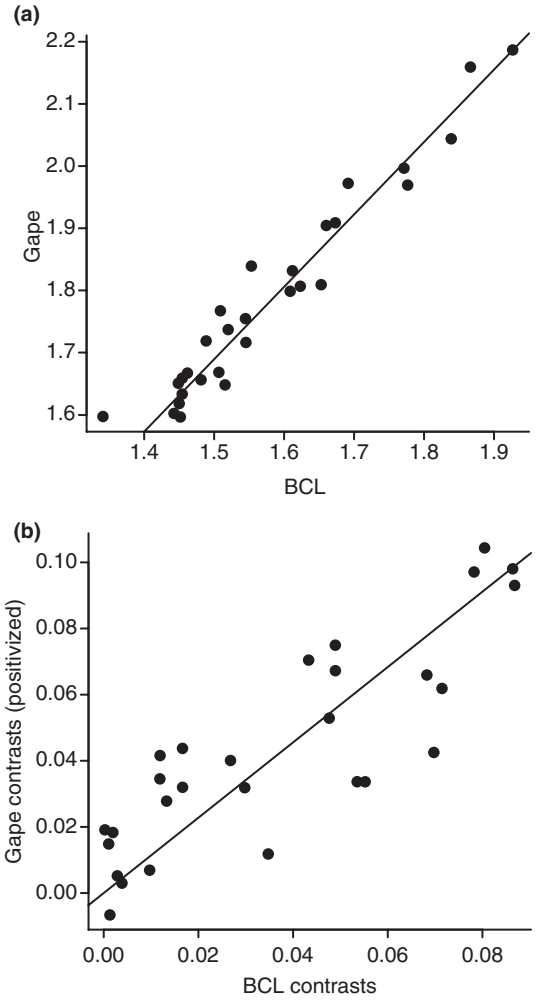

Fig. 1 Scatter plots showing MA slopes for (a) log gape distance on log basicranial length and (b) gape contrasts on basicranial length contrasts.

Table 3 Bite forces (N) for intrinsic loads and strain energy values (J) for intrinsic and extrinsic loading of the three finite element models.

	Taxon		
	Felis lybica	*Neofelis nebulosa*	*Panthera leo*
Bite force			
Bilateral	240.8	237.4	228.5
Unilateral	466.2	465.2	441.6
Intrinsic load strain energy			
Bilateral	0.082	0.124	0.102
Unilateral	0.104	0.152	0.120
Extrinsic load strain energy			
Pull-back	0.138	0.202	0.192
Lateral shake	0.412	0.812	0.854
Bilateral canine	0.066	0.100	0.087
Unilateral canine	0.073	0.120	0.105

towards positive allometry in gape distance (Fig. 1b). A slope test based on the contrasts data also accepts this slope as significantly > 1 (slope test, $r = 0.372$, $P = 0.05$).

Bite performance

Variation in bite force among the three FE models is inversely proportional to jaw length and gape distance. The shortest-jawed felid, the wild cat, produced the highest bite forces for the muscle force used, and the longest-jawed felid, the lion, produced the lowest bite forces (Table 3). Overall, however, the absolute differences in bite force magnitudes among the four models were small, with maximum differences of 12 N for bilateral biting and 25 N for unilateral biting.

Skull strength

The three models exhibited some general similarities in mechanical performance during intrinsic loading (Fig. 2). In all three, stresses were highest in the rostrum, jaw joint and zygomatic arches. Nevertheless, there were also pronounced differences among the models. Skull strength increased with increasing felid size. During bilateral biting (Fig. 2a–c), the lion was least stressed and the wild cat was most stressed, with the clouded leopard intermediately stressed. Plots of stress values taken from the midline along the dorsal surface of the skulls (Fig. 3a) show that the wild cat and clouded leopard exhibited irregular stress magnitudes, with sharp stress gradients. The lion exhibited smoother, lower stress gradients, with stress decreasing anteroposteriorly. During unilateral biting (Fig. 2d–f), stresses were concentrated on the working, or biting side of the rostrum and the balancing, or opposing side jaw joint for all models. Overall, performance was similar to that observed for bilateral biting, with higher and less evenly distributed stresses in the wild cat (Fig. 3b). Stress magnitudes were intermediate in the clouded leopard and lowest in the lion.

Extrinsic loading resulted in similar patterns to those observed during intrinsic loading (Fig. 4). In all cases, the wild cat exhibited the highest stress values, the

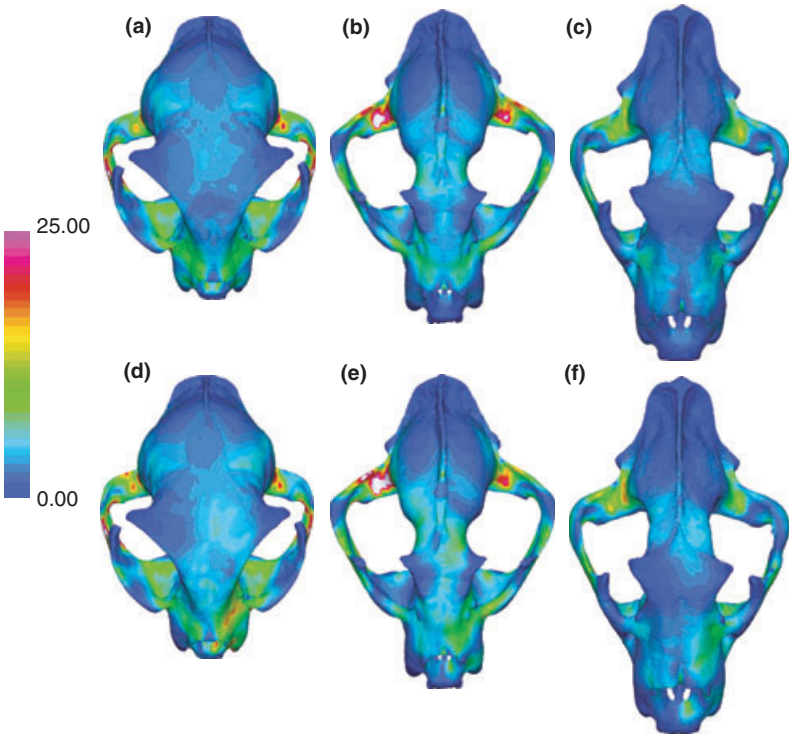

Fig. 2 Contour plots of von Mises stress during bilateral (a–c) and unilateral (d–f) canine biting. Warm colours indicate high stress; cool colours indicate low stress. Taxa are *Felis lybica* (a,d), *Neofelis nebulosa* (d,e) and *Panthera leo* (c,f).

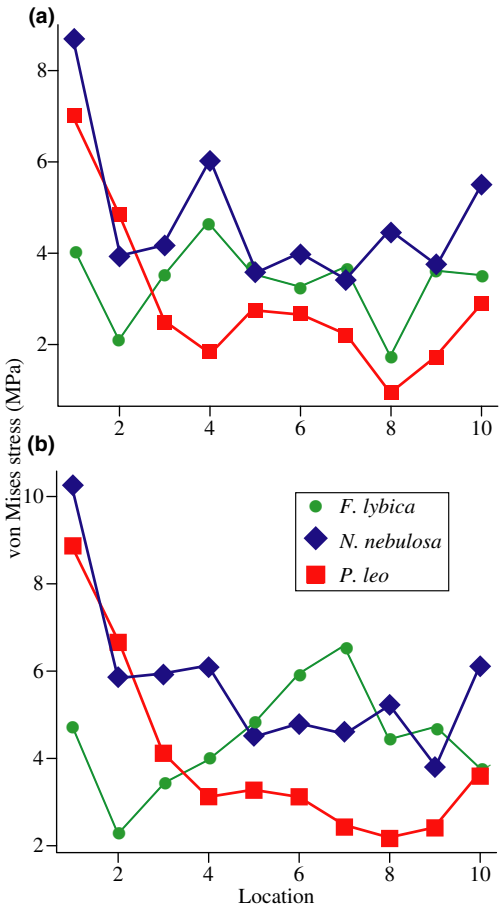

Fig. 3 Plots of von Mises stress taken from the dorsal midline of the skull models during (a) bilateral and (b) unilateral canine biting. 1 is anterior, 10 is posterior.

clouded leopard was intermediate and the lion was least stressed.

Work efficiency

In contrast with the results for skull strength, work efficiency did not increase with felid size. The wild cat exhibited the lowest strain energy values for all loading conditions (Table 3), indicating that its skull shape is most work efficient. The clouded leopard and lion exhibited similar strain energy values, suggesting similar work efficiency, although the lion was slightly more efficient in most load cases (lion = 78–105% of clouded leopard values, mean = 89%; Table 3).

Discussion

Our results show that larger felids have both absolutely and relatively larger gape distances than small felids. The importance of gape for predatory performance in felids relates directly to the mode of prey capture in these carnivores. As predominantly solitary ambush predators, felids kill their prey using a single bite either to the nape, throat or muzzle (Ewer, 1973; Leyhausen, 1979), and are therefore restricted to prey with throats or necks that can fit between the canine teeth (Kiltie, 1984, 1988). Larger gape distances should increase the range of prey sizes that can be taken by large felids. This is corroborated by field studies of predatory behaviour. Although large carnivores do not focus exclusively on large prey, they do take a wider range of prey sizes (Radloff & Du Toit, 2004) and prefer larger prey (Hayward & Kerley, 2005). This predatory strategy contrasts with other hypercarnivorous carnivorans such as canids or hyaenids, which use multiple shallow, tearing bites in combination with pack hunting to subdue and kill large prey, and therefore exhibit different patterns of cranial shape variation (Slater *et al.*, 2009).

The presence of other gape-enhancing features in large cat crania lends additional support to the importance of gape for predatory ecology in felids. Large felids also exhibit ventrally displaced jaw joints and palates that are dorsally rotated relative to the basicranium (Slater & Van Valkenburgh, 2008). Both of these features should contribute to further increases in total gape distance. A ventrally displaced jaw joint increases the maximum possible angle of jaw rotation, and a dorsally rotated palate increases total clearance of the canines for a given angle of rotation. Because our measurements of gape distance did not incorporate variation in these features, we suspect that we have underestimated gape distance in larger felids. Muscle architecture is also likely to play an important role in determining maximum gape distance. Future work measuring gape in vivo from living felids will help corroborate our findings.

Lengthening the jaw for increased gape compromises the mechanical advantage of the jaw musculature, resulting in lower bite forces at the canine teeth. The smallest felid, the wild cat, produced the largest bite force for the muscle force used, whereas the largest felid, the lion, produced the smallest bite force, although the magnitude of these differences was small. Under a null hypothesis of geometric similarity, bite force would be expected to scale to body mass$^{2/3}$, as force production scales isometrically with the physiological cross-sectional area (PCSA) of the jaw muscles (Emerson & Bramble, 1993). Estimates based on dry skull measurements support this hypothesis in Carnivora, although bite force quotients (bite force adjusted for body size) are slightly higher in felids that take large prey (Christiansen & Wroe, 2007). These estimates were derived from measurements of the areas occupied by jaw musculature and measurements of jaw lever arms (Thomason, 1991). Increases in muscle PCSA in larger felids may compensate for the loss of leverage arising from positive allometry of the facial skeleton. Alternatively, leverage might be maintained through increasing the length of the coronoid process of the mandible, the jaw in-lever

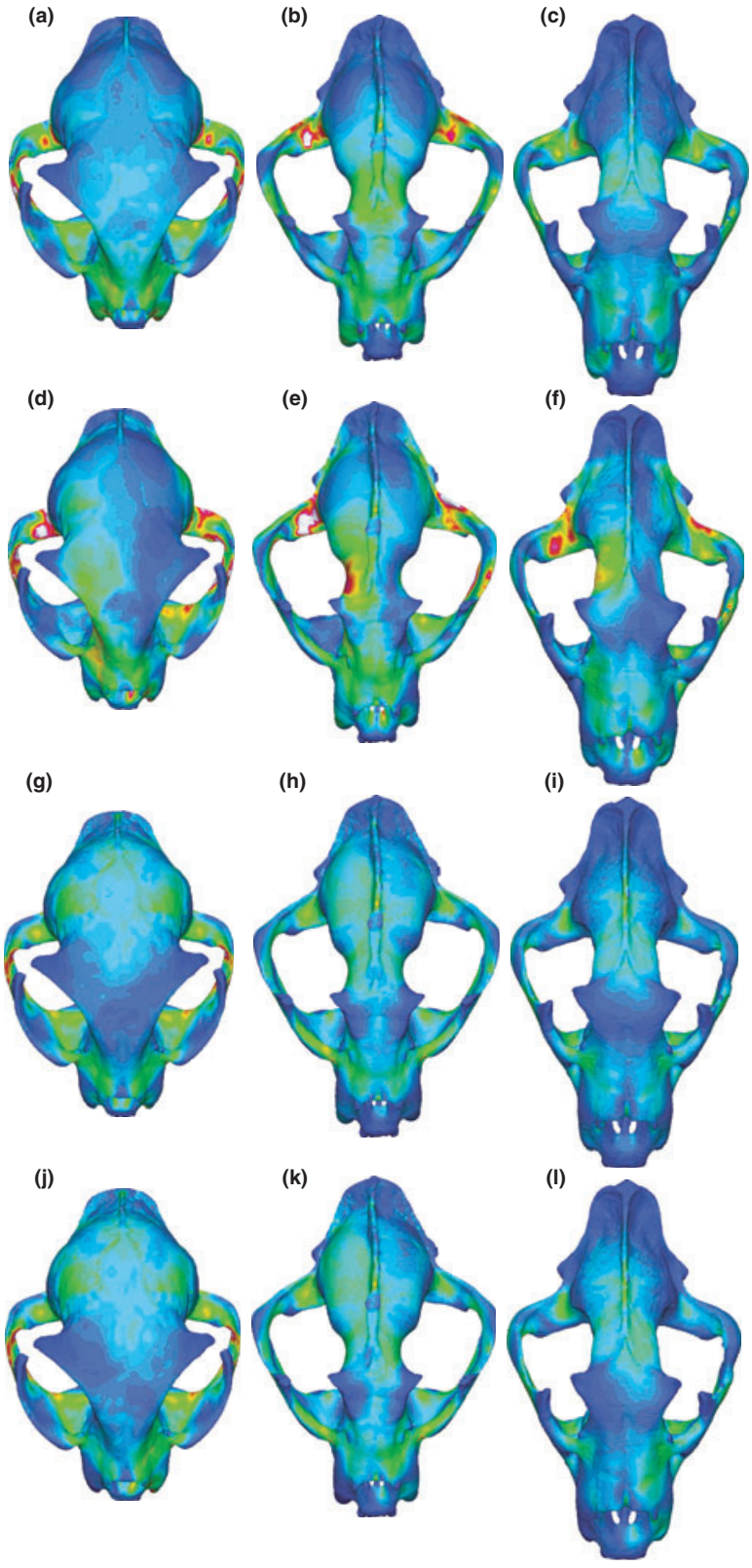

Fig. 4 Contour plots of von Mises stress during extrinsic load cases: (a–c) pull back; (d–f) lateral shake; (g–i) bending; and (j–l) torsion. Taxa are *Felis lybica* (left), *Neofelis nebulosa* (centre) and *Panthera leo* (right). As in Fig. 3, cool colours indicate low stress; hot colours indicate high stress. The scale is the same as Fig. 2.

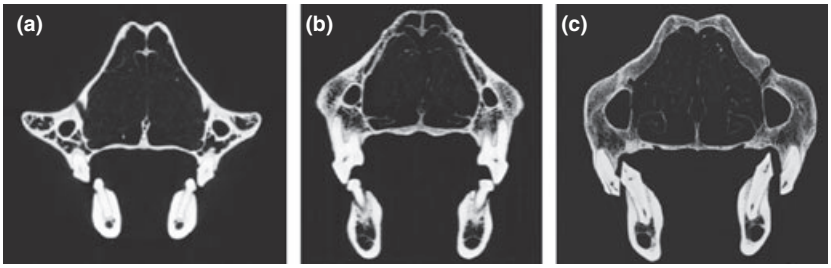

Fig. 5 Transverse CT slices through the rostra of the three species modelled. All slices are taken at the upper fourth premolar (carnassial). (a) *Felis lybica*, (b) *Neofelis nebulosa* and (c) *Panthera leo*.

(Meachen-Samuels & Van Valkenburgh, 2009). Either way, the near uniformity of bite forces produced in scaled FE models, combined with data from dry-skull estimates of bite force supports the conclusion that felids maintain relative bite force with increasing size, rather than increasing it.

Large cat skulls appear to be overbuilt with respect to the intrinsic loads that they generate while biting. However, other forces act on the skulls of predators during the act of prey killing, and these forces offer an explanation for our results. Maximum prey size increases with body size among felids, and large felids regularly take prey much larger than themselves (Van Valkenburgh & Hertel, 1998; Radloff & Du Toit, 2004; Hayward & Kerley, 2005; Meachen-Samuels & Van Valkenburgh, 2009). Even moderately sized prey can generate considerable forces when struggling in a predator's jaws (Preuschoft and Witzel, 2005). Large prey can take up to 10 min to kill (Schaller, 1972) and are therefore likely to pose a significant challenge to the skulls of large felids. FE models of the large cat crania performed substantially better than the small cat under all extrinsic loading conditions. This finding suggests that strengthening the cranium in response to extrinsic loads incurred by struggling prey, rather than to those incurred by intrinsic forces, may be more important in the evolution of cranial strength in felids.

Although previous studies have focused on the strengthening effects of changes in external skull geometry (e.g. Covey & Greaves, 1994; Slater *et al.*, 2009), the superior strength and mechanical efficiency of large cat skulls seems to result mostly from a change in internal geometry, or an increase in the amount of bone used to construct the skull. Bone is a metabolically expensive material (Currey, 2002) and is therefore expected to be distributed sparingly. In fact, theoretical studies of skull mechanics have assumed minimal use of bone (e.g. Thomason, 1991; Covey & Greaves, 1994). Although we scaled our models to common surface area, substantial variation in model volume persisted, and the lion model volume was twice that of the wild cat model (Table 2). These differences are apparent when bone thickness is compared in the rostra of the three species (Fig. 5). Large felids are likely to encounter more unpredictable loading of the skull when hunting large prey, and thicker skull bone provides one way of compensating for the loss of skull strength that results from elongation of the facial skeleton to maximize gape.

In contrast with our findings about cranial strength, our data suggest a fundamental trade-off between maximizing gape and work efficiency of the cranium in felids. Work efficiency is a measure of energy lost to deformation and describes the amount of strain energy stored in a skull during biting. Although the lion's cranium was strongest overall, it showed poor work efficiency. Strain energy values were high relative to the wild cat under both intrinsic and extrinsic loading conditions. This is somewhat surprising, as selection should favour shapes that maximize work efficiency in biological structures made of ductile materials such as bone. This pattern is seen in canids, where the crania of species that specialize on large prey were both stronger and more work efficient than the crania of generalists or small prey specialists (Slater *et al.*, 2009). Felids present a rather different case. Although canids that take large prey exhibit shorter jaws to produce increased bite forces, felids that take large prey exhibit lengthening of the jaw to increase gape distance. Although large felids are able to compensate for decreased strength by incorporating additional bone in their skulls, a longer jaw ultimately results in a less stiff structure that undergoes more deformation during biting (Thomason, 1991). Thus it seems that in the evolution of large felids, biomechanically efficient crania and high bite forces have been traded for the ability to handle large, metabolically valuable prey (Carbone *et al.*, 1999).

Acknowledgments

We thank the following for access to specimens: E. Westwig (American Museum of Natural History, New York), L. Gordon (National Museum of Natural History, Washington, D.C.), K. Molina (Donald R. Dickey Collection, UCLA), J. Dines (Los Angeles County Museum of Natural History), P. Gaubert (Musee National d'Histoire Naturel, Paris), P. Jenkins and D. Hills (Natural History Museum London). We are extremely grateful to E. Dumont for advice and discussion of ideas and methods. W. Ary and L. Louis provided assistance with model construction. E. Dumont, G. Dyke, A. Galligan, S. Price, J. Tseng and an anonymous reviewer provided valuable criticism of earlier versions of this manuscript. We thank the high-resolution CT facility at UT Austin for

scanning specimens. This work was supported by NSF DDIG 0709792 and a UCLA EEB Research Grant to GJS and NSF IOB 0517748 to BVV.

References

Arnold, S.J. 1983. Morphology, performance and fitness. *Am. Zool.* **23**: 347–361.

Bailey, T.N. 1993. *The African Leopard: Ecology and Behavior of a Solitary Felid*. Columbia University Press, New York.

Carbone, C., Mace, G.M., Roberts, S.C. & Macdonald, D.W. 1999. Energetic constraints on the diet of terrestrial carnivores. *Nature* **402**: 286–288.

Christiansen, P. 2008. Evolution of skull and mandible shape in cats. *PLoS ONE* **3**: e2807.

Christiansen, P. & Adolfssen, J.S. 2005. Bite forces, canine strength and skull allometry in carnivores (Mammalia, Carnivora). *J. Zool. Lond.* **266**: 133–151.

Christiansen, P. & Wroe, S. 2007. Bite forces and evolutionary adaptations to feeding ecology in carnivores. *Ecology* **88**: 347–358.

Cook, S.D., Weinstein, A.M. & Klawitter, J.J. 1982. A 3-dimensional finite element analysis of a porous rooted Co-Cr-Mo alloy dental implant. *J. Dent. Res.* **61**: 25–29.

Covey, D.S.G. & Greaves, W.S. 1994. Jaw dimensions and torsion resistance during canine biting in the Carnivora. *Can. J. Zool.* **72**: 1055–1060.

Currey, J.D. 2002. *Bones: Structure and Mechanics*. Princeton University Press, Princeton, NJ.

Davis, D.D. 1955. Masticatory apparatus in the Spectacled bear *Tremarctos ornatus*. *Fieldiana: Zool.* **37**: 25–46.

Dumont, E.R., Piccirillo, J. & Grosse, I.R. 2005. Finite element analysis of biting behavior and bone stress in the facial skeleton of bats. *Anat. Rec. A.* **283**: 319–330.

Dumont, E.R., Grosse, I.R. & Slater, G.J. 2009. Requirements for comparing the performance of finite element models of biological structures. *J. Theor. Biol.* **256**: 96–103.

Emerson, S.B. & Bramble, D.M. 1993. Scaling, allometry, and skull design. In: *The Skull. Volume 3: Functional and Evolutionary Mechanisms* (J. Hanken & B.K. Hall, eds), pp. 384–421. Chicago University Press, Chicago.

Emerson, S.B. & Radinsky, L. 1980. Functional analysis of sabertooth cranial morphology. *Paleobiology* **6**: 295–312.

Emerson, S.B., Greene, H.W. & Charnov, E.L. 1994. Allometric aspects of predator-prey interactions. In: *Ecological Morphology: Integrative Organismal Biology* (P.C. Wainwright & S.M. Reilly, eds), pp. 123–139. Chicago University Press, Chicago.

Ewer, R.F. 1973. *The Carnivores*. Weidenfeld and Nicolson, London, UK.

Garland, T., Harvey, P.H. & Ives, A.R. 1992. Procedures for the analysis of comparative data using phylogenetically independent contrasts. *Sys. Biol.* **41**: 18–32.

Gould, S.J. 1966. Allometry and size in ontogeny and phylogeny. *Biol. Rev.* **41**: 587–640.

Gould, S.J. 1977. *Ontogeny and Phylogeny*. Harvard University Press, Cambridge, MA.

Grosse, I.R., Dumont, E.R., Coletta, C. & Tolleson, A. 2007. Techniques for modeling muscle-induced forces in finite element models of skeletal structures. *Anat. Rec. A* **290**: 1069–1088.

Hayward, M.W. & Kerley, G.I.H. 2005. Prey preferences of the lion (*Panthera leo*). *J. Zool. Lond.* **267**: 309–322.

Herring, S.W. 1975. Adaptations for gape in the hippopotamus and its relatives. *Forma et Functio* **8**: 85–100.

Johnson, W.E., Eizirik, E., Pecon-Slattery, J., Murphy, W.J., Antunes, A., Teeling, E. & O'Brien, S.J. 2005. The Late Miocene radiation of modern Felidae: a genetic assessment. *Science* **311**: 73–77.

Kiltie, R.A. 1984. Size ratios among sympatric neotropical cats. *Oecologia* **61**: 411–416.

Kiltie, R.A. 1988. Interspecific size regularities in tropical felid assemblages. *Oecologia* **76**: 97–105.

Leyhausen, P. 1979. *Cat Behaviour: Predatory and Social Behaviour of Domestic and Wild Cats*. Garland STPM Press, New York.

Maddison, W.P. & Maddison, D.R. 2009. Mesquite: a modular system for evolutionary analysis. Version 2.6. http://mesquiteproject.org.

McHenry, C.R., Wroe, S., Clausen, P.D., Moreno, K. & Cunningham, E. 2007. Supermodeled sabercat, predatory behavior in Smilodon fatalis revealed by high-resolution 3D computer simulation. *Proc. Natl Acad. Sci. USA* **104**: 16010–16015.

Meachen-Samuels, J. & Van Valkenburgh, B. 2009. Craniodental indicators of prey size preference in the Felidae. *Biol. J. Linn. Soc.* **96**: 784–799.

Nalla, R.K., Kinney, J.H. & Ritchie, R.O. 2003. Mechanistic failure criteria for the failure of human cortical bone. *Nature Materials* **2**: 164–168.

Preuschoft, H. & Witzel, U. 2005. Functional shape of the skull in vertebrates: Which forces determine skull morphology in lower primates and ancestral synapsids? *Anat. Rec. A* **283A**: 402–413.

Paradis, E., Claude, J. & Strimmer, K. 2004. APE: analyses of phylogenetics and evolution in R language. *Bioinformatics* **20**: 289–290.

R Development Core Team (2008). *R: A Language and Environment for Statistical Computing*. R Foundation for Statistical Computing, Vienna, Austria. ISBN 3-900051-07-0, URL http://www.R-project.org.

Radinsky, L. 1984. Basicranial axis length *v.* skull length in analysis of carnivore skull shape. *Biol. J. Linn. Soc.* **22**: 31–41.

Radloff, F.G.T. & Du Toit, J.T. 2004. Large predators and their prey in a southern African savanna: a predator's size determines its prey range. *J. Animal. Ecol.* **73**: 410–423.

Rasband, W.S. 2006. *ImageJ, v. 1.37*. U. S. National Institutes of Health, Bethesda, MD, USA, http://rsb.info.nih.gov/ij/.

Schaller, G.B. 1972. *The Serengeti Lion. A Study of Predator-Prey Relations*. The University of Chicago Press, Chicago, IL.

Schmidt-Nielsen, K. 1984. *Scaling: Why is Animal Size So Important?* Cambridge University Press, Cambridge, UK.

Slater, G.J. & Van Valkenburgh, B. 2008. Long in the tooth: the evolution of sabertooth cat cranial shape. *Paleobiology* **34**: 403–419.

Slater, G.J., Dumont, E.R. & Van Valkenburgh, B. 2009. Implications of predatory specialization for cranial form and function in canids. *J. Zool. Lond.* **278**: 181–188.

Strait, D.S., Wang, Q., Dechow, P.C., Ross, C.F., Richmond, B.G., Spencer, M.A. & Patel, B.A. 2005. Modeling elastic properties in finite element analysis: how much precision is needed to produce an accurate model? *Anat. Rec. A* **283**: 275–287.

Thomason, J.J. 1991. Cranial strength in relation to estimated biting strength in some mammals. *Can. J. Zool.* **69**: 2326–2333.

Thompson, J.W. 1942. *On Growth and Form, the Complete Revised Edition*. Dover, New York.

Turnbull, W.D. 1970. Mammalian masticatory apparatus. *Fieldiana, Geol.* **18**: 149–356.

Van Valkenburgh, B. 1988. Trophic diversity in past and present guilds of large predatory mammals. *Paleobiology* **14**: 155–173.

Van Valkenburgh, B. & Hertel, F. 1998. The decline of North American predators during the late Pleistocene. In: *Quaternary Paleozoology in the Northern Hemisphere* (J.J. Saunders, B.W. Styles & G.F. Baryshnikov, eds), pp. 357–374. Ill. State Mus. Sci. Papers, Vol. X XVII.

Van Valkenburgh, B. & Ruff, C.B. 1987. Canine tooth strength and killing behaviour in large carnivores. *J. Zool. Lond.* **222**: 379–397.

Verrue, V., Dermaut, L. & Verhegghe, B. 2001. Three-dimensional finite element modelling of a dog skull for the simulation of initial orthopaedic displacements. *Eur. J. Orthod.* **23**: 517–527.

Wainwright, P.C. 1994. Functional morphology as a tool in ecological research. In: *Ecological Morphology: Integrative Organismal Biology* (P.C. Wainwright & S.M. Reilly, eds), pp. 42–59. Chicago University Press, Chicago.

Warton, D.I., Wright, I.J., Falster, D.S. & Westoby, M. 2006. Bivariate line-fitting methods for allometry. *Biol. Rev.* **81**: 259–291.

Wayne, R.K. 1986. Cranial morphology of domestic and wild canids – the influence of development on morphological change. *Evolution* **40**: 243–261.

Wroe, S. 2008. Cranial mechanics compared in extinct marsupial and extant African lions using a finite-element approach. *J. Zool. Lond.* **274**: 332–339.

Wroe, S., Clausen, P., McHenry, C., Moreno, K. & Cunningham, E. 2007a. Computer simulation of feeding behaviour in the thylacine and dingo as a novel test for convergence and niche overlap. *Proc. R. Soc. Lond. B Biol. Sci.* **274**: 2819–2828.

Wroe, S., Moreno, K., Clausen, P., McHenry, C. & Curnoe, D. 2007b. High-resolution three-dimensional computer simulation of hominid cranial mechanics. *Anat. Rec. A* **290**: 1248–1255.

Received 9 June 2009; revised 19 August 2009; accepted 2 September 2009